J. Fluid Mech. (2018), *vol.* 854, *pp.* 449–473.
doi:10.1017/jfm.2018.578

Integral properties of turbulent-kinetic-energy production and dissipation in turbulent wall-bounded flows

Tie Wei†

Department of Mechanical Engineering, New Mexico Institute of Mining and Technology, Socorro, NM 87801, USA

(Received 16 February 2018; revised 14 May 2018; accepted 17 July 2018; first published online 10 September 2018)

Turbulent-kinetic-energy (TKE) production $\mathscr{P}_k = R_{12}(\partial U/\partial y)$ and TKE dissipation $\mathscr{E}_k = \nu\langle(\partial u_i/x_k)(\partial u_i/x_k)\rangle$ are important quantities in the understanding and modelling of turbulent wall-bounded flows. Here U is the mean velocity in the streamwise direction, u_i or u, v, w are the velocity fluctuation in the streamwise x- direction, wall-normal y- direction, and spanwise z-direction, respectively; ν is the kinematic viscosity; $R_{12} = -\langle uv\rangle$ is the kinematic Reynolds shear stress. Angle brackets denote Reynolds averaging. This paper investigates the integral properties of TKE production and dissipation in turbulent wall-bounded flows, including turbulent channel flows, turbulent pipe flows and zero-pressure-gradient turbulent boundary layer flows (ZPG TBL). The main findings of this work are as follows. (i) The global integral of TKE production is predicted by the RD identity derived by Renard & Deck (*J. Fluid Mech.*, vol. 790, 2016, pp. 339–367) as $\int_0^\delta \mathscr{P}_k\,\mathrm{d}y = U_b u_\tau^2 - \int_0^\delta \nu(\partial U/\partial y)^2\,\mathrm{d}y$ for channel flows, where U_b is the bulk mean velocity, u_τ is the friction velocity and δ is the channel half-height. Using inner scaling, the identity for the global integral of the TKE production in channel flows is $\int_0^{\delta^+} \mathscr{P}_k^+\mathrm{d}y^+ = U_b^+ - \int_0^{\delta^+}(\partial U^+/\partial y^+)^2\,\mathrm{d}y^+$. In the present work, superscript $+$ denotes inner scaling. At sufficiently high Reynolds number, the global integral of the TKE production in turbulent channel flows can be approximated as $\int_0^{\delta^+} \mathscr{P}_k^+\,\mathrm{d}y^+ \approx U_b^+ - 9.13$. (ii) At sufficiently high Reynolds number, the integrals of TKE production and dissipation are equally partitioned around the peak Reynolds shear stress location y_m: $\int_0^{y_m} \mathscr{P}_k\,\mathrm{d}y \approx \int_{y_m}^{\delta} \mathscr{P}_k\,\mathrm{d}y$ and $\int_0^{y_m} \mathscr{E}_k\,\mathrm{d}y \approx \int_{y_m}^{\delta} \mathscr{E}_k\,\mathrm{d}y$. (iii) The integral of the TKE production $\mathcal{I}_{\mathscr{P}_k}(y) = \int_0^y \mathscr{P}_k\,\mathrm{d}y$ and the integral of the TKE dissipation $\mathcal{I}_{\mathscr{E}_k}(y) = \int_0^y \mathscr{E}_k\,\mathrm{d}y$ exhibit a logarithmic-like layer similar to that of the mean streamwise velocity as, for example, $\mathcal{I}^+_{\mathscr{P}_k}(y^+) \approx (1/\kappa)\,\ln(y^+) + C_{\mathscr{P}}$ and $\mathcal{I}^+_{\mathscr{E}_k}(y^+) \approx (1/\kappa)\,\ln(y^+) + C_{\mathscr{E}}$, where κ is the von Kármán constant, $C_{\mathscr{P}}$ and $C_{\mathscr{E}}$ are addititve constants. The logarithmic-like scaling of the global integral of TKE production and dissipation, the equal partition of the integrals of TKE production and dissipation around the peak Reynolds shear stress location y_m and the logarithmic-like layer in the integral of TKE production and dissipation are intimately related. It is known that the peak Reynolds shear stress location y_m scales with a meso-length scale $l_m = \sqrt{\delta\nu/u_\tau}$. The equal partition of the integral of the TKE production anddissipation

† Email address for correspondence: tie.wei@nmt.edu

around y_m underlines the important role of the meso-length scale l_m in the dynamics of turbulent wall-bounded flows.

Key words: boundary layer structure, boundary layers

1. Introduction

Beginning with Prandtl in 1904, turbulent wall-bounded flows have been intensively investigated by numerous researchers. Reviews of the topic can be found in Cantwell (1981), Robinson (1991), Gad-el Hak & Bandyopadhyay (1994), Fernholz & Finley (1996), Klewicki (2010), Marusic *et al.* (2010*b*), Smits, McKeon & Marusic (2011), Jiménez (2013), Smits & Marusic (2013), and Marusic, Baars & Hutchins (2017). The present work focuses on turbulent-kinetic-energy (TKE) production and dissipation, and specifically on the integral properties of TKE production and dissipation.

Better knowledge of TKE production $\mathscr{P}_k = R_{12}(\partial U/\partial y)$ and TKE dissipation $\mathscr{E}_k = \nu\langle(\partial u_i/x_k)(\partial u_i/x_k)\rangle$ can shed light on how turbulence is (re)generated and sustained. In this work, U represents the mean velocity in the streamwise direction x, and u, v represent the fluctuating velocity component in the streamwise direction x and the wall-normal direction y, and $R_{12} = -\langle uv\rangle$ is the kinematic Reynolds shear stress. Angle brackets denote averaging. While the balance of the TKE budget equation is commonly presented in numerical simulation of turbulent wall-bounded flows, as by Eggels *et al.* (1994), Abe, Kawamura & Matsuo (2001), Hoyas & Jiménez (2008), Wu & Moin (2009), Jiménez *et al.* (2010), the integral of TKE production and dissipation has received less attention.

Panton (2001) pointed out the important role of TKE production in the generation of Reynolds stress and self-sustaining turbulence in the near-wall region. It is well known that the peak TKE production occurs within the viscous buffer layer at $y^+ \approx 12$ (Fernholz & Finley 1996). In the present work, superscript $^+$ denotes inner scaling. The inner-scaled distance, y^+, from the wall, is $y^+ = y/(\nu/u_\tau)$ where u_τ is the friction velocity. Plotting the pre-multiplied TKE production on semilogarithmic axes, Marusic, Mathis & Hutchins (2010*a*) have shown that the main contribution to the bulk TKE production comes from the near-wall region at low Reynolds number. At sufficiently high Reynolds number the logarithmic region dominates TKE production, as shown in Marusic *et al.* (2010*a*), Bernardini, Pirozzoli & Orlandi (2014), Pirozzoli, Bernardini & Orlandi (2016) and Renard & Deck (2016).

Orlandi (1997) derived a decomposition of the TKE production into two parts, one containing the streamwise component of the fluctuating Lamb vector and the other in a divergence form. Using direct numerical simulation (DNS) data, Bernardini *et al.* (2014) examined Orlandi's decomposition of TKE production. They proposed a scaling for the TKE production and offered an explanation for the mixed scaling $\sqrt{u_\tau U_\infty}$ for the streamwise velocity variance $\langle uu\rangle$, where U_∞ is the free streamwise velocity of zero-pressure-gradient turbulent boundary layer flows (ZPG TBLs).

Pirozzoli *et al.* (2016) have investigated the global TKE production for the mean streamwise velocity and scalar. They found that the near-wall region is characterized by nearly equal values of velocity and scalar production, and the global velocity dissipation is found to exceed the global dissipation of the scalar. The difference was attributed to the pressure term in the velocity equation, consistent with the analogy proposed by Abe & Antonia (2009).

Laadhari (2007) examined the Reynolds number dependence of the dissipation of the mean kinetic energy and TKE in wall-bounded flow. He found that the mean part reaches a constant value at sufficiently high Reynolds number, while the turbulent part follows a logarithmic law. Laadhari (2007) pointed out that the logarithmic law of friction can be obtained without any assumption on the mean velocity distribution.

Recently, Abe & Antonia (2016) examined the integrals of the mean and TKE dissipation rates using DNS data from turbulent channel flow. They established a logarithmic dependence of the integrated turbulent energy dissipation rate for $300 < \delta^+ < 10^4$, and found that the dependence is intimately linked to the logarithmic skin friction law. The scaling of the turbulent energy dissipation rate in the inner region, outer region and overlap region were examined. Abe & Antonia (2017) have extended the studies on the integration of the transport equations for the mean and turbulent parts of the scalar dissipation rate, and have obtained a simple relation for the bulk mean scalar and the wall transfer coefficient.

Renard & Deck (2016) derived an identity that decomposes the mean skin friction coefficient into a laminar part and a turbulent part. One motive for Renard and Deck's work was to improve the FIK identity, a decomposition of the mean skin friction coefficient derived by Fukagata, Iwamoto & Kasagi (2002). The Renard and Deck (RD) identity was also independently derived by Abe & Antonia (2016). While the FIK identity and the RD identity focus on the decomposition of the mean skin friction coefficient, here we show that the RD identity in fact reveals a very important property of the TKE production, that is, the global integral of the TKE production.

The rest of the paper is organized as follows. In § 2, we present the RD identity in the form of the global integral of TKE production for turbulent channel flows, turbulent pipe flows and ZPG TBL. In § 3.1 we briefly present the distribution of $\mathscr{P}_k$ and $\mathscr{E}_k$. In § 3.2 the RD identity equations are verified using DNS and experimental data from turbulent channel flows, turbulent pipe flows and ZPG TBL. In § 3.3 we briefly review the scaling for the peak Reynolds shear stress location and meso-length scale. In § 3.4 we present the pre-multiplied TKE production and dissipation. In § 3.5 we show the partition of the integral of the TKE production and dissipation around the peak Reynolds shear stress location y_m. In § 3.6 we present the integral profiles of the TKE production and dissipation.

2. The RD identity and the global integral of the TKE production

Using the mean streamwise kinetic-energy budget equation in an absolute reference frame, Renard & Deck (2016) derived a decomposition of the mean skin friction coefficient C_f in turbulent wall-bounded flows. For channel flows, the RD identity can be written as

$$C_f = \frac{2}{U_b^3}\int_0^\delta \nu \left(\frac{\partial U}{\partial y}\right)^2 \mathrm{d}y + \frac{2}{U_b^3}\int_0^\delta R_{12}\frac{\partial U}{\partial y}\,\mathrm{d}y, \quad \text{RD identity}, \tag{2.1}$$

where δ is the channel half-height, the mean skin friction coefficient is defined as $C_f = \tau_w/(0.5\rho U_b^2) = 2u_\tau^2/U_b^2$ and $U_b = (\int_0^\delta U\,\mathrm{d}y)/\delta$ is the bulk mean velocity. Renard & Deck (2016) have thoroughly examined the contribution of turbulence to the mean skin friction. While they focused on the mean skin friction, here we examine the RD identity from the perspective of the global integral of the TKE production. For completeness, we will briefly derive the RD identity using a simplified approach.

The simplified derivation starts from the mean momentum balance (MMB) equation for fully developed turbulent channel flow:

$$0 = \frac{u_\tau^2}{\delta} + \nu\frac{\partial^2 U}{\partial y^2} + \frac{\partial R_{12}}{\partial y}, \tag{2.2}$$

where u_τ^2/δ comes from the mean pressure force $-(1/\rho)(\mathrm{d}P/\mathrm{d}x)$ (see Pope 2001). The corresponding boundary conditions are

$$y = 0 \text{ (wall)}: \quad U = 0, \quad R_{12} = 0, \quad \nu\frac{\partial U}{\partial y} = u_\tau^2; \tag{2.3a–c}$$

$$y = \delta \text{ (centreline)}: \quad U = U_c, \quad R_{12} = 0. \tag{2.4a,b}$$

Integrating the MMB equation (2.2) in the wall-normal direction and applying boundary conditions yields a relation for the total shear stress, viscous shear stress plus Reynolds shear stress, as

$$\nu\frac{\partial U}{\partial y} + R_{12} = u_\tau^2 - \frac{u_\tau^2}{\delta}y. \tag{2.5}$$

The integral of TKE production can be obtained in two steps. Step one is to multiply the MMB equation (2.2) by a weight function U

$$0 = \frac{u_\tau^2}{\delta}U + \nu\frac{\partial^2 U}{\partial y^2}U + \frac{\partial R_{12}}{\partial y}U. \tag{2.6}$$

In step two, the weighted MMB equation (2.6) is integrated in the wall-normal direction y to produce

$$0 = \frac{u_\tau^2}{\delta}\int_0^y U\,\mathrm{d}y + \left\{\nu\frac{\partial U}{\partial y}U - \nu\int_0^y\left(\frac{\partial U}{\partial y}\right)^2\mathrm{d}y\right\} + \left\{R_{12}U - \int_0^y R_{12}\frac{\partial U}{\partial y}\,\mathrm{d}y\right\}. \tag{2.7}$$

Note that integration by parts was applied to the second and third terms in (2.6), and no-slip boundary conditions were applied for U and R_{12} at the channel wall.

Substituting the relation for $\nu(\partial U/\partial y) + R_{12}$ in (2.5), the integrated equation (2.7) can be rearranged as

$$\int_0^y \mathscr{P}_k\,\mathrm{d}y = \left\{u_\tau^2 U - u_\tau^2\frac{\left(yU - \displaystyle\int_0^y U\,\mathrm{d}y\right)}{\delta}\right\} - \nu\int_0^y\left(\frac{\partial U}{\partial y}\right)^2\mathrm{d}y. \tag{2.8}$$

For brevity, we denote the TKE production term as $\mathscr{P}_k = R_{12}(\partial U/\partial y)$. The global integral identity for TKE production is obtained by setting $y = \delta$ in the integral equation (2.8)

$$\int_0^\delta \mathscr{P}_k\,\mathrm{d}y = u_\tau^2 U_b - \nu\int_0^\delta\left(\frac{\partial U}{\partial y}\right)^2\mathrm{d}y. \tag{2.9}$$

It can be easily shown that the identity equation (2.9) is the RD identity equation (2.1).

In the study of turbulent wall-bounded flows, u_τ and ν are often used to scale the mean velocity, Reynolds shear stress and wall-normal distance as $U^+ = U/u_\tau$, $R_{12}^+ = R_{12}/u_\tau^2$ and $y^+ = yu_\tau/\nu$. This procedure is commonly referred to as 'inner scaling'. The inner-scaled integral equation (2.8) can be expressed as

$$\int_0^{y^+} \mathscr{P}_k^+ \,\mathrm{d}y^+ = \left\{ U^+ - \frac{y^+U^+ - \displaystyle\int_0^{y^+} U^+ \,\mathrm{d}y^+}{\delta^+} \right\} - \int_0^{y^+} \left(\frac{\partial U^+}{\partial y^+}\right)^2 \mathrm{d}y^+, \tag{2.10}$$

and the global integral identity equation (2.9) in inner scaling can be expressed as

$$\int_0^{\delta^+} \mathscr{P}_k^+ \,\mathrm{d}y^+ = U_b^+ - \int_0^{\delta^+} \left(\frac{\partial U^+}{\partial y^+}\right)^2 \mathrm{d}y^+, \tag{2.11}$$

where the inner-scaled TKE production is $\mathscr{P}_k^+ = R_{12}^+(\partial U^+/\partial y^+)$. In other words, the RD identity states that the sum of the global integrals of $(\partial U^+/\partial y^+)^2$ and the TKE production $\mathscr{P}_k^+$ always equals U_b^+ in a channel flow, regardless of the Reynolds number. The identity equation (2.9) for the global integral of TKE production was first presented by Laadhari (2007). Although Laadhari started with the dissipation equation for the kinetic energy, equating the TKE production to dissipation in turbulent channel flow, he essentially used the mean momentum balance equation to obtain the identity equation. Here the identity equation is derived in a more straightforward fashion.

Due to the geometric shape, the global integral identity for the TKE production in turbulent pipe flows is (see appendix B for more details)

$$\frac{1}{R^+}\int_0^{R^+} \mathscr{P}_k^+ r^+ \,\mathrm{d}r^+ = U_b^+ - \frac{1}{R^+}\int_0^{R^+} \left(\frac{\partial U^+}{\partial r^+}\right)^2 r^+ \,\mathrm{d}r^+, \tag{2.12}$$

where $\mathscr{P}_k^+ = R_{12}^+(\partial U^+/\partial r^+)$ for turbulent pipe flow.

The global integral identity for the TKE production in ZPG TBL is (see appendix A for more details)

$$\begin{aligned}\int_0^{\delta^+} \mathscr{P}_k^+ \,\mathrm{d}y^+ \;=\; & U_\infty^+ - \int_0^{\delta^+} \left(\frac{\partial U^+}{\partial y^+}\right)^2 \mathrm{d}y^+ + \left\{ \int_0^{\delta^+} U^+ \left[U^+ \frac{\partial V^+}{\mathrm{d}y^+} - V^+ \frac{\partial U^+}{\mathrm{d}y^+} \right] \mathrm{d}y^+ \right. \\ & \left. - U_\infty^+ \int_0^{\delta^+} \left[U^+ \frac{\partial V^+}{\mathrm{d}y^+} - V^+ \frac{\partial U^+}{\mathrm{d}y^+} \right] \mathrm{d}y^+ \right\}. \end{aligned} \tag{2.13}$$

The identity equations for the global TKE production in turbulent channel flow, turbulent pipe flow and ZPG TBL have similar form, but there are subtle differences. For example, it is known that the profiles of the mean velocity and Reynolds shear stress of channel and pipe flows are similar, but there are subtle differences, especially in the wake region (see Jiménez *et al.* 2009; Mathis *et al.* 2009*b*; Monty *et al.* 2009, and Ng *et al.* 2011). Given the difference in geometry and the ensuing difference in the integration, the global identities for channel flow and pipe flow will not be the same, as we will show in the following.

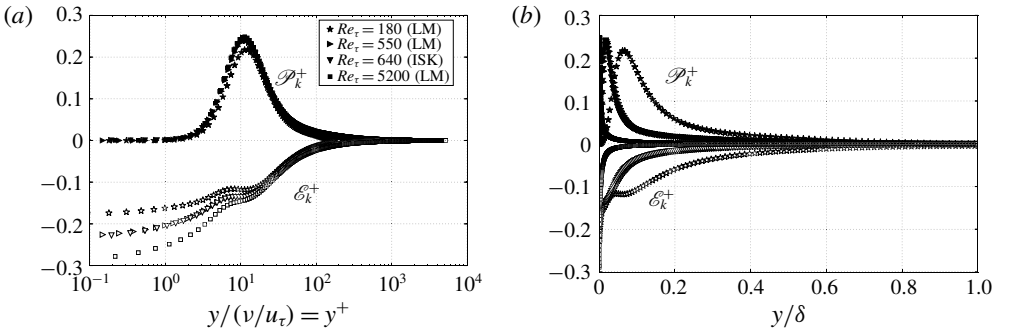

FIGURE 1. TKE production and dissipation versus wall-normal distance. (*a*) Inner-scaled wall-normal distance y^+. (*b*) Outer-scaled wall-normal distance y/δ. Data are from independent DNS studies by Iwamoto *et al.* (2002) and Lee & Moser (2015).

3. Experimental and numerical data

The calculation of the TKE production $\mathscr{P}_k$ requires data on the mean streamwise velocity gradient $\partial U/\partial y$ and the kinematic Reynolds shear stress R_{12}. In physical experiments, the spatial resolution is limited, especially in the near-wall region, where the gradient $\partial U/\partial y$ varies rapidly. Moreover, in high Reynolds number physical experiments, the first data point of R_{12} is often beyond the peak Reynolds shear stress location. Thus, it is challenging to obtain TKE production $\mathscr{P}_k$ data in physical experiments, especially in the near-wall region of high Reynolds number flows. The measurement of the TKE dissipation $\mathscr{E}_k$ in physical experiments is even more difficult. The scarcity of the TKE production and dissipation data from physical experiments is one of the reasons why their integrals have not been widely studied in the past.

During the past three decades, however, numerical simulations, especially direct numerical simulation, have provided high quality data for $\mathscr{P}_k$ and $\mathscr{E}_k$. At the same time, higher resolution probes have been developed to obtain data in the near-wall region of high Reynolds number flows (see, for example, Vallikivi, Hultmark & Smits 2015). The present work would not have been possible without the aid of the high quality DNS data and experimental data generously shared by the researchers. Here, we use DNS and high resolution experimental data to investigate the integral properties of TKE production and dissipation, including the global integral, partition of the integrals, and shapes of the integral profiles.

3.1. *TKE production and dissipation distribution*

TKE production $\mathscr{P}_k$ and dissipation $\mathscr{E}_k$ profiles have been commonly presented in DNS studies of turbulent wall-bounded flows (see, for example, Eggels *et al.* 1994; Abe *et al.* 2001; Hoyas & Jiménez 2008; Wu & Moin 2009; Jiménez *et al.* 2010). For the convenience of readers, figure 1 presents $\mathscr{P}_k$ and $\mathscr{E}_k$ versus wall-normal distance from two independent DNS studies of turbulent channel flows by Iwamoto, Suzuki & Kasagi (2002) and Lee & Moser (2015). The agreement between the DNS of Lee & Moser (2015) at $Re_\tau = 550$ and the DNS of Iwamoto *et al.* (2002) at $Re_\tau = 640$ indicates the high quality of the simulations.

In figure 1(*a*) the wall-normal distance is inner scaled as $y^+ = y/(\nu/u_\tau)$. To better show the near-wall region, the data are plotted on semilogarithmic axes. To show the

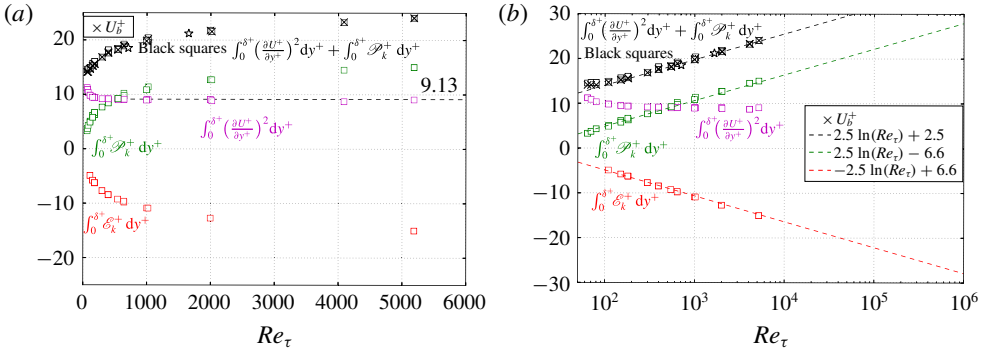

FIGURE 2. (Colour online) Reynolds number dependence of the global integral of $\int_0^{\delta^+}(\partial U^+/\partial y^+)^2\,\mathrm{d}y^+$ (magenta squares), $\int_0^{\delta^+}\mathscr{P}_k^+\,\mathrm{d}y^+$ (green squares) and $\int_0^{\delta^+}\mathscr{E}_k^+\,\mathrm{d}y^+$ (red squares) in turbulent channel flows. Also shown are the sum of $\int_0^{\delta^+}(\partial U^+/\partial y^+)^2\,\mathrm{d}y^+$ and $\int_0^{\delta^+}\mathscr{P}_k^+\,\mathrm{d}y^+$ (black squares), the U_b^+ from DNS (black $\times$) and U_b^+ from experimental measurement (black star) by Wei & Willmarth (1989). (*a*) On linear–linear axes. (*b*) On semilogarithmic axes. DNS data are from four independent studies: Abe *et al.* (2001), Iwamoto *et al.* (2002), Lee & Moser (2015), Pirozzoli *et al.* (2016).

trend in the outer region, figure 1(*b*) presents TKE production and dissipation versus the outer-scaled location y/δ.

Three notable features of figure 1(*a*) are as follows. (i) The inner-scaled TKE production $\mathscr{P}_k^+$ peaks at $y^+ \approx 12$ with a maximum value of about $\mathscr{P}_{k,max}^+ \approx 0.25$, with no apparent Reynolds number dependence (the $Re_\tau = 180$ case clearly has a low Reynolds number effect). (ii) The inner-scaled TKE dissipation at the wall $\mathscr{E}_k^+(y=0)$ clearly increases with Reynolds number. (iii) The TKE production $\mathscr{P}_k^+$ and dissipation $\mathscr{E}_k^+$ are not always in equilibrium. For example, the balance of the TKE budget equation in the viscous sublayer is between the dissipation $\mathscr{E}_k^+$ and the viscous diffusion term. However, the viscous diffusion, turbulent transport and pressure velocity correlation terms in the TKE budget equation only redistribute TKE among different layers, and the global integral of these transport terms can be shown to be zero in turbulent channel flow and turbulent pipe flows. Therefore, the global integral of TKE production and dissipation must have the same magnitude, but with opposite signs. The global identity for the TKE production should also apply to the global integral of the TKE dissipation.

The balance of the TKE budget equation among different terms is commonly presented in DNS studies of turbulent wall-bounded flows, as in Bernardini *et al.* (2014) and Lee & Moser (2015), and is not discussed here. The focus of this work is on the integral properties of the TKE production and dissipation, that is, the area under the $\mathscr{P}_k^+$ curve and $\mathscr{E}_k^+$ curve in figure 1(*b*).

3.2. *Global integral of TKE production and dissipation*

Using R_{12} and U data from four independent DNS studies of turbulent channel flows by Abe *et al.* (2001), Iwamoto *et al.* (2002), Lee & Moser (2015) and Pirozzoli *et al.* (2016), the global integrals $\int_0^{\delta^+}\mathscr{P}_k^+\,\mathrm{d}y^+$ and $\int_0^{\delta^+}(\partial U^+/\partial y^+)^2\,\mathrm{d}y^+$ are calculated and presented in figure 2 as a function of Reynolds number. Also shown in the figures

is the global integral $\int_0^{\delta^+} \mathscr{E}_k^+ \,\mathrm{d}y^+$ calculated from the DNS data of TKE dissipation term. To illustrate the global integral identity equation (2.11) for channel flows, the bulk mean velocity U_b^+ from DNS is also plotted in figure 2. As a test of accuracy, the experimental measurement of U_b^+ by Wei & Willmarth (1989) is plotted in the figure, and can be seen to agree well with the DNS data.

Figure 2 shows that the sum of $\int_0^{\delta^+} (\partial U^+/\partial y^+)^2 \,\mathrm{d}y^+$ and $\int_0^{\delta^+} \mathscr{P}_k^+ \,\mathrm{d}y^+$ (black open squares in the plot) agrees very well with U_b^+ (black $\times$ or star in the plot), and this supports the validity of the global integral identity equation (2.11).

Figure 2 shows that in low Reynolds number turbulent channel flow, $\int_0^{\delta^+} (\partial U^+/\partial y^+)^2 \,\mathrm{d}y^+ > \int_0^{\delta^+} \mathscr{P}_k^+ \,\mathrm{d}y^+$ (in a laminar channel flow, $\int_0^{\delta^+} (\partial U^+/\partial y^+)^2 \,\mathrm{d}y^+ = U_b^+$). However, as Reynolds number increases, $\int_0^{\delta^+} (\partial U^+/\partial y^+)^2 \,\mathrm{d}y^+$ decreases to a constant value of approximately 9.13 for $Re_\tau > 300$. This constant value is consistent with the results of Laadhari (2007) and Abe & Antonia (2016). Thus, at sufficiently high Reynolds number, the global integral of the TKE production and dissipation in turbulent channel flows can be approximated as

$$\int_0^{\delta^+} \mathscr{P}_k^+ \,\mathrm{d}y^+ = \int_0^{\delta^+} \mathscr{E}_k^+ \,\mathrm{d}y^+ \approx U_b^+ - 9.13 \quad \text{or} \quad \int_0^{\delta} \mathscr{P}_k \,\mathrm{d}y = \int_0^{\delta} \mathscr{E}_k \,\mathrm{d}y \approx U_b u_\tau^2 - 9.13 u_\tau^3. \tag{3.1a,b}$$

To date, the highest U_b^+ obtained in superpipe experiments by Hultmark *et al.* (2012, 2013) is around $U_b^+ \sim 35$, so the contribution of $\int_0^{\delta^+} (\partial U^+/\partial y^+)^2 \,\mathrm{d}y^+ \approx 9.13$ is not negligible in the identity equation (3.1). However, at infinite Reynolds number, $U_b^+ \gg 9.13$ and $\int_0^{\delta^+} \mathscr{P}_k^+ \,\mathrm{d}y^+ = \int_0^{\delta^+} \mathscr{E}_k^+ \,\mathrm{d}y^+ \approx U_b^+$.

To better show the Reynolds number dependence, figure 2(*b*) presents the data on semilogarithmic axes. In figure 2(*b*) a logarithmic function is used to approximate the Reynolds number dependence of the inner-scaled bulk mean velocity as $U_b^+ \approx 2.5 \ln(Re_\tau) + 2.5$. From (3.1), the approximate function for the global integral of the TKE production and dissipation becomes

$$\int_0^{\delta^+} \mathscr{P}_k^+ \,\mathrm{d}y^+ = -\int_0^{\delta^+} \mathscr{E}_k^+ \,\mathrm{d}y^+ \approx 2.5 \ln(Re_\tau) - 6.6. \tag{3.2}$$

Given the complicated nature of turbulent wall-bounded flows, it is unlikely that the exact Reynolds number dependence of U_b^+ is a simple logarithmic function, but it is not the purpose of this work to determine the best fitting function or parameters for the Reynolds number dependence. Figure 2(*b*) shows that the increase of U_b^+, $\int_0^{\delta^+} \mathscr{P}_k^+ \,\mathrm{d}y^+$ and $\int_0^{\delta^+} \mathscr{E}_k^+ \,\mathrm{d}y^+$ with Reynolds number is in fact nearly logarithmic. Similar logarithmic functions have been used by Laadhari (2007), Zanoun, Nagib & Durst (2009) and Abe & Antonia (2016) to approximate the bulk mean velocity in high Reynolds number turbulent channel flow.

Figure 3 presents the Reynolds number dependence of the global integral results in turbulent pipe flows. As shown in the figures, the sum of $(1/R^+) \int_0^{R^+} (\partial U^+/\partial r^+)^2 r^+ \,\mathrm{d}r^+$ and $(1/R^+) \int_0^{R^+} \mathscr{P}_k^+ r^+ \,\mathrm{d}r^+$ agrees excellently with the U_b^+ data, and this strongly supports the global integral identity equation (2.12). The deviation of the superpipe data from the trend is caused by the spatial resolution in the near-wall region. At such a high Reynolds number, the first data point is close to or beyond the peak Reynolds shear stress location. In the superpipe experiments by Vallikivi *et al.*

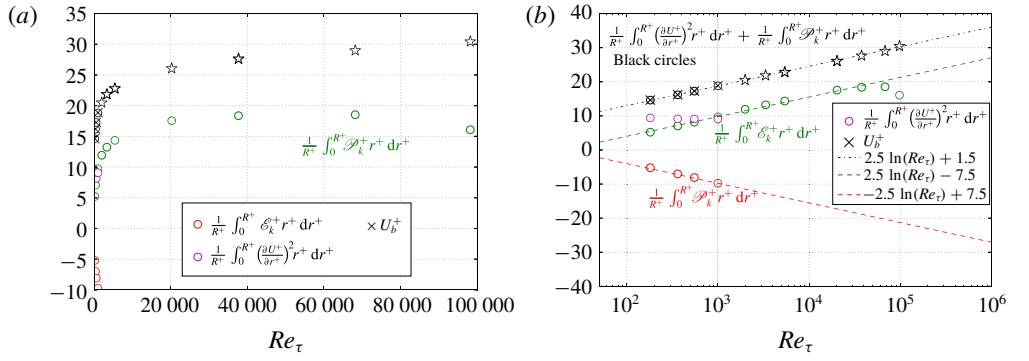

FIGURE 3. (Colour online) Reynolds number dependence of the global integral of $(1/R^+)\int_0^{R^+}(\partial U^+/\partial r^+)^2 r^+\,\mathrm{d}r^+$ (magenta circles), $(1/R^+)\int_0^{R^+}\mathscr{P}_k^+ r^+\,\mathrm{d}r^+$ (green circles) and $(1/R^+)\int_0^{R^+}\mathscr{E}_k^+ r^+\,\mathrm{d}r^+$ (red circles) in turbulent pipe flows. Also shown are the sum of $(1/R^+)\int_0^{R^+}(\partial U^+/\partial r^+)^2 r^+\,\mathrm{d}r^+$ and $(1/R^+)\int_0^{R^+}\mathscr{P}_k^+ r^+\,\mathrm{d}r^+$ (black circles), U_b^+ from DNS (black $\times$) by El Khoury *et al.* (2013) and U_b^+ from superpipe (black star) by Hultmark *et al.* (2012, 2013). (*a*) On linear–linear axes. (*b*) On semilogarithmic axes.

(2015), the Reynolds shear stress R_{12} is not measured. For the calculation of $\mathscr{P}_k$, R_{12} is calculated indirectly using $\partial U/\partial y$ and the once-integrated mean momentum balance equation (see appendix B).

Figure 4 shows the global integral results for ZPG TBL. Due to the advection term (the last two integrals) in (2.13), the sum of $\int_0^{\delta^+}(\partial U^+/\partial y^+)^2\,\mathrm{d}y^+$ and $\int_0^{\delta^+}\mathscr{P}_k^+\,\mathrm{d}y^+$ will be smaller than U_∞^+, as shown in the figure, but figure 4 shows that the difference is small, indicating that the mean advection has a minor role in the global balance of the TKE budget. The deviation of the experimental data at $Re_\tau \approx 10\,000$ is caused by the spatial resolution of data points in the experiments of De Graaff & Eaton (2000).

To sum up, the global integral identity of the TKE production (2.11)–(2.13) has been verified with high resolution experimental and DNS data from turbulent channel flows, pipe flows and ZPG TBL. Next, we will present the partition of the integral of the TKE production and dissipation in turbulent wall-bounded flows. We find that at sufficiently high Reynolds number, the integrals of the TKE production and dissipation are equally partitioned around the peak Reynolds shear stress location y_m. Given the importance of y_m and meso-scaling in the partition of the integral of TKE production and dissipation, we will briefly review the meso-layer and meso-scaling before presenting the partition of the integrals.

3.3. *Meso-layer, meso-length scale and peak location of Reynolds shear stress*

The concept of a meso-layer has been proposed in a number of studies, including Long & Chen (1981), Afzal (1982, 1984), Sreenivasan & Sahay (1997), Wosnik, Castillo & George (2000) and Wei *et al.* (2005). For example, in Wei *et al.* (2005) a four-layer structure is proposed for turbulent wall-bounded flows, based on the force balance of the mean momentum balance equation. Their Layer III (the meso-layer) centres around the peak Reynolds shear stress location y_m.

A meso-length scale for turbulent channel/pipe and ZPG TBL flows has been proposed as the geometric mean of the inner length scale $l_\nu = \nu/u_\tau$ and the outer

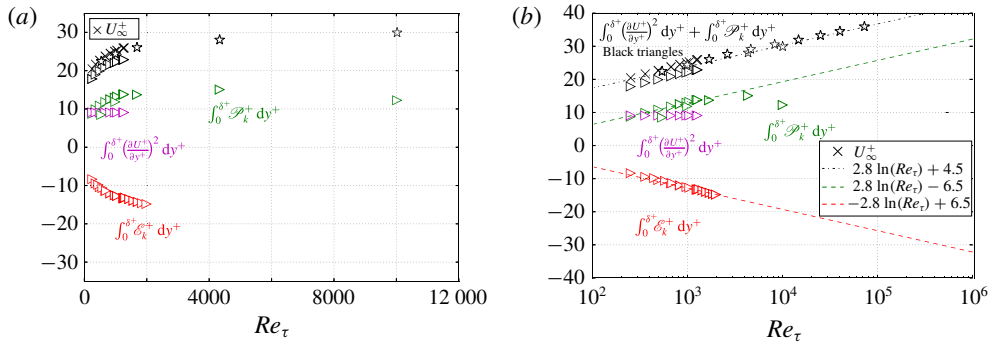

FIGURE 4. (Colour online) Reynolds number dependence of the global integral of $\int_0^{\delta^+}(\partial U^+/\partial y^+)^2\,\mathrm{d}y^+$ (magenta triangles), $\int_0^{\delta^+}\mathscr{P}_k^+\,\mathrm{d}y^+$ (green triangles) and $\int_0^{\delta^+}\mathscr{E}_k^+\,\mathrm{d}y^+$ (red triangles) in ZPG TBL. Also shown are the sum of $\int_0^{\delta^+}(\partial U^+/\partial y^+)^2\,\mathrm{d}y^+ + \int_0^{\delta^+}\mathscr{P}_k^+\,\mathrm{d}y^+$ (black triangles), U_∞^+ from DNS (black $\times$) and U_∞^+ from experimental measurement (black asterisk) by De Graaff & Eaton (2000), Vallikivi *et al.* (2015). (*a*) On linear–linear axes. (*b*) On semilogarithmic axes. DNS data are from two independent studies by Simens *et al.* (2009) and Schlatter & Örlü (2010).

length scale $l_o=\delta$, as $l_m=\sqrt{\delta\nu/u_\tau}$ (Fife *et al.* 2005*a*,*b*; Wei *et al.* 2005). Meso-length scale l_m has been advocated as a fundamental length scale in turbulent channel/pipe flow and ZPG TBL, like the l_ν and l_o (Fife *et al.* 2005*a*,*b*; Wei *et al.* 2005). It has long been known that the peak Reynolds shear stress location y_m scales as $y_m=O(\sqrt{\delta\nu/u_\tau})$ (see, for example, Long & Chen 1981; Sreenivasan 1989; Sreenivasan & Sahay 1997; Wei *et al.* 2005). Thus, the peak Reynolds shear stress location y_m scales as the meso-length scale.

The meso-length scaling is defined as

$$\frac{y}{l_m}=\frac{y}{\sqrt{\delta\nu/u_\tau}}=\frac{y^+}{\sqrt{\delta^+}}. \tag{3.3}$$

Given the spatial resolution limitation inherent in physical experiments, it has been challenging to determine y_m precisely. However, during the past thirty years, more DNS data at higher Reynolds numbers, and higher resolution experimental data, have made it possible to determine more precisely the Reynolds number dependence of y_m. Figure 5 shows the Reynolds number dependence of the meso-scaled peak location y_m/l_m. The experimental and numerical data in figure 5 offer strong evidence that at sufficiently high Reynolds number the peak Reynolds shear stress location y_m scales as the meso-length scale: $y_m=O(l_m)$.

Figure 5 shows that the peak Reynolds shear stress location y_m in turbulent channel flows is approximately $y_m\approx 1.5l_m$ or $y_m^+\approx 1.5\sqrt{\delta^+}$ for $Re_\tau>2000$. The peak Reynolds shear stress location in ZPG TBL is slightly larger, at $y_m\approx 2.4l_m$ or $y_m^+\approx 2.4\sqrt{\delta^+}$. In the 1980s, Long & Chen (1981) proposed a similar scaling but with a numerical factor of 1.87, and Sreenivasan (1989) suggested a numerical factor of 2.0. Given the spatial resolution of the instrumentation available then, and the Reynolds number range of the data, these predictions are remarkably close to the recent DNS and high resolution experimental data shown in figure 5.

One motivation for the present work is to assess the role of the meso-layer and meso-length scale in the partition of the integrals of TKE production and dissipation.

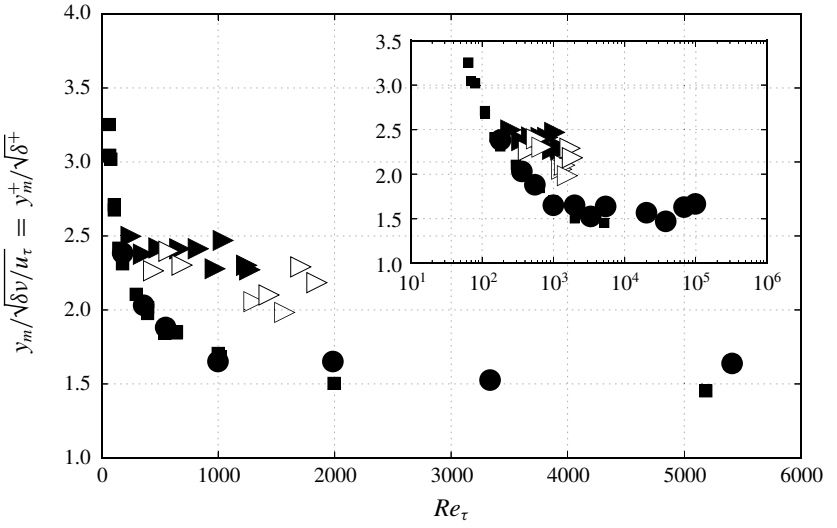

FIGURE 5. Dependence of Reynolds shear stress peak location y_m on Reynolds numbers. Squares are channel flow data from DNS of Abe *et al.* (2001), Iwamoto *et al.* (2002), Lee & Moser (2015), circles are pipe flow data from DNS of El Khoury *et al.* (2013) and superpipe by Hultmark *et al.* (2012, 2013) and triangles are ZPG-TBL data from DNS by Schlatter & Örlü (2010) (filled triangles) and Simens *et al.* (2009) (open triangles). Note Reynolds shear stress R_{12} is not directly measured in the superpipe, but calculated indirectly as $R_{12}^+ = 1 - y^+/R^+ - \partial U^+/\partial y^+$ (see appendix B for more details).

In figure 6 we present the distribution of the TKE production and dissipation versus the meso-scaled distance from the wall, to complement the inner-scaled distance and the outer-scaled distance presented in figure 1. The peak location of TKE production in meso-scaling becomes smaller with increasing Reynolds number. This is not surprising, as the peak location of the TKE production scales with inner scaling.

3.4. *Pre-multiplied TKE production and dissipation*

To better show the near-wall region, it is common to plot the wall-normal distance on a logarithmic scale. For the convenience of depicting the area under the curve (its integral) on semilogarithmic axes, the TKE production and dissipation have been pre-multiplied by the wall-normal distance, because the derivative of a logarithmic function has the following property:

$$\mathrm{d}\log_{10}(y) = \frac{1}{\ln(10)}\frac{1}{y}\mathrm{d}y. \tag{3.4}$$

Thus the area under the pre-multiplied TKE production and dissipation curves on semilogarithmic axes equals the integrals of TKE production and dissipation. For the inner-scaled y^+ and meso-scaled y/l_m, the integrals of TKE production (or dissipation) can be written, respectively, as

$$\int_0^{\delta^+} \mathscr{P}_k^+ \,\mathrm{d}y^+ = \int_{\log_{10}(y_1^+)}^{\log_{10}(\delta^+)} [\ln(10)] y^+ \mathscr{P}_k^+ \,\mathrm{d}(\log_{10} y^+), \tag{3.5}$$

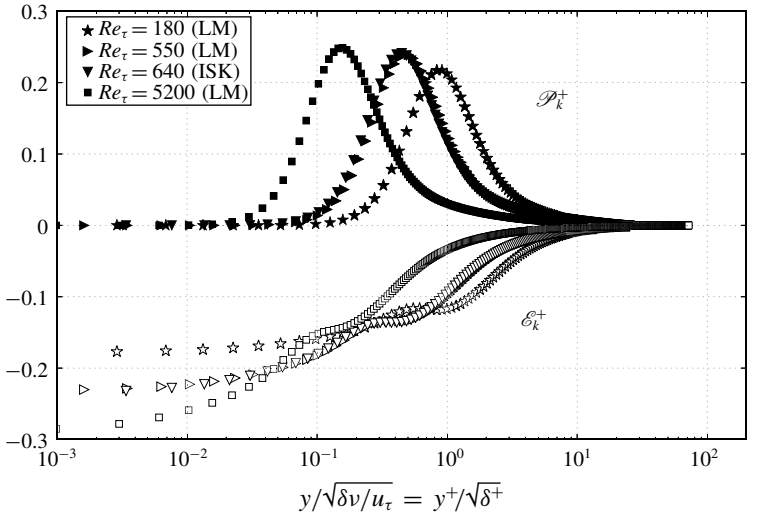

FIGURE 6. TKE production and dissipation versus meso-scaled distance from the wall y/l_m. Data from DNS of channel flow Iwamoto *et al.* (2002) and Lee & Moser (2015).

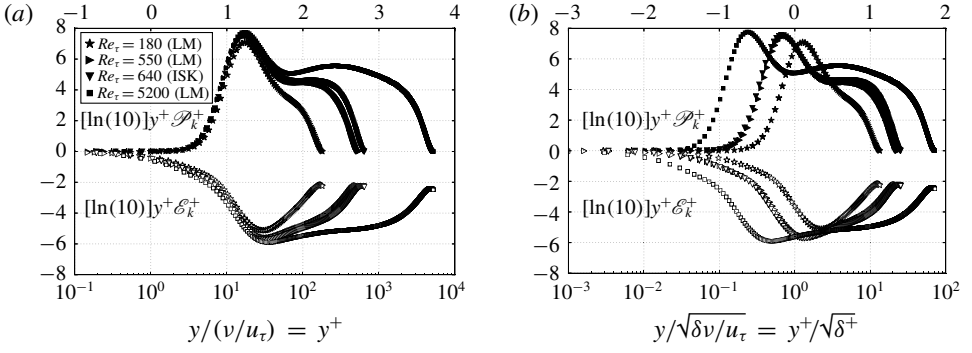

FIGURE 7. Pre-multiplied TKE production and dissipation versus distance from the wall on semilogarithmic axes. (*a*) Distance from the wall is inner scaled y^+. (*b*) Distance from the wall is meso-scaled y/l_m. The xticks on bottom denote values of y^+ or y/l_m and xticks on top denote values of $\log_{10}(y^+)$ or $\log_{10}(y/l_m)$.

$$\int_0^{\delta^+} \mathscr{P}_k^+ \,\mathrm{d}y^+ = \int_{\log_{10}(y_1^+/\sqrt{\delta^+})}^{\log_{10}(\sqrt{\delta^+})} [\ln(10)]y^+\mathscr{P}_k^+ \,\mathrm{d}\left(\log_{10}\left(\frac{y^+}{\sqrt{\delta^+}}\right)\right), \tag{3.6}$$

where y_1 is the location of the first data point above the surface. As $\log(0)$ is undefined, the first data point y_1 should not be at the wall. In practice, the first data point is at a small distance from the wall.

In figure 7(*a*) the pre-multiplied TKE production and dissipation are plotted versus the inner-scaled distance from the wall y^+ on semilogarithmic axes. For convenience, the xticks on the bottom show values of y^+ and the xticks on the top show values of $\log_{10} y^+$. As in figure 1(*a*), the pre-multiplied TKE production also peaks within the viscous buffer layer at $y^+ \approx 12$.

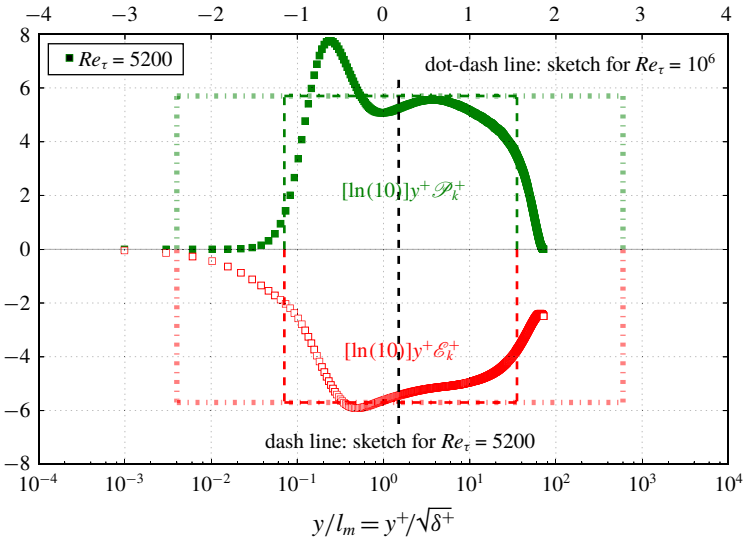

FIGURE 8. (Colour online) Sketch approximating the integral of TKE production and dissipation at high Reynolds number. Dashed curves approximate the area under the pre-multiplied TKE production and dissipation curves of DNS data at $Re_\tau = 5300$ by Lee & Moser (2015). The dot-dashed curves are approximations for a higher Reynolds number at $Re_\tau = 10^6$. The trend will be similar as Reynolds number increases further. The vertical dashed black line denotes the peak Reynolds shear stress location $y_m/l_m \approx 1.5$, as shown in figure 5.

Figure 7 shows that as Reynolds number increases the pre-multiplied TKE production and dissipation approach a plateau away from the wall, before dropping sharply towards the channel centre. It has been observed that at sufficiently high Reynolds number, say $Re_\tau > 20\,000$, a second bump appears away from the wall in the pre-multiplied TKE production profile. For example, using a composite mean velocity profile and the corresponding Reynolds shear stress profile proposed by Perry, Marusic & Jones (2002), Marusic *et al.* (2010*a*) sketched the pre-multiplied TKE production profiles $y^+\mathscr{P}_k^+$ for different Reynolds numbers. The value of the plateau is approximately $y^+\mathscr{P}_k^+ \approx 2.5$. Their sketch for $Re_\tau = 10^6$ shows a smaller second bump away from the wall (Marusic *et al.* 2010*a*). The second bump is also observed in the plot by Pirozzoli *et al.* (2016).

In figure 7(*b*), the pre-multiplied TKE production and dissipation are plotted versus the meso-scaled distance from the wall y/l_m on semilogarithmic axes. The advantage of the meso-scaled length scale is shown in figure 8, in which the area under the curves of the pre-multiplied TKE production and dissipation is approximated by a rectangle.

In figure 8 the dashed rectangle approximates the integral of the TKE production and dissipation at $Re_\tau = 5300$ of Lee & Moser (2015), and the dot-dashed rectangle is an extrapolation for a higher Reynolds number at $Re_\tau = 10^6$. The height of the rectangle is approximately $\ln(10)y^+\mathscr{P}_k^+ \approx 5.7$, which is consistent with the value used in the sketch of Marusic *et al.* (2017), differing by a factor of $\ln(10)$.

The width of the rectangle in figure 8 can be approximated as $\log_{10}(\delta^+)$ (see the xticks on the top of figure 8). Thus the area under the curves of the pre-multiplied TKE production and dissipation can be approximated as $5.7\log_{10}(\delta^+) \approx 2.5\ln(Re_\tau)$.

		y_1	y_m	δ
Inner scaling	y^+	1	$\sqrt{\delta^+}$	δ^+
	$\log_{10}(y^+)$	0	$\frac{1}{2}\log_{10}(\delta^+)$	$\log_{10}(\delta^+)$
Meso-scaling	$\frac{y}{\sqrt{\delta\nu/u_\tau}}$	$\frac{1}{\sqrt{\delta^+}}$	1	$\sqrt{\delta^+}$
	$\log_{10}\left(\frac{y}{\sqrt{\delta\nu/u_\tau}}\right)$	$-\frac{1}{2}\log_{10}(\delta^+)$	0	$\frac{1}{2}\log_{10}(\delta^+)$

TABLE 1. Partition of boundary layer around the meso-layer. For convenience, the first data point is taken as $y_1^+ = 1$. (One can choose other values for y_1. For example, if $y_1^+ = 0.1$, then $\log_{10}(0.1) = -1$, and $\log_{10}(0.1/\sqrt{\delta^+}) \approx -0.5\log_{10}(\delta^+) - 1$. As $\delta^+ \to \infty$, the constant -1 becomes negligible. Furthermore, as y_1 becomes smaller than 0.1, the pre-multiplied TKE production and dissipation quickly approach 0.)

This approximation is consistent with the Reynolds number dependence in the global integral identity equation $\int_0^{\delta^+} \mathscr{P}_k^+ \,\mathrm{d}y^+ = \int_0^{\delta^+} \mathscr{E}_k^+ \,\mathrm{d}y^+ \approx U_b^+ - 9.13$ and the data for $U_b^+ \approx 2.5\ln(Re_\tau) + 2.5$, as shown in figure 2(*b*).

The vertical dashed line at $y/l_m = 1.5$ in figure 8 indicates the peak Reynolds shear stress location, as shown in figure 5. Figure 8 shows that the width of the rectangle on both sides of y_m is of the order of $0.5\log_{10}(\delta^+)$ (see the xticks on the top).

The equal partition of the integral of the TKE production and dissipation around y_m can also be explained using table 1. The ranges of boundary layer around y_m, in meso-scaling, are $O((\log_{10}(\delta^+))/2)$ on both sides. Assuming A_k for the height of the rectangle that approximates the pre-multiplied TKE production or dissipation, the area or the integral of TKE production and dissipation between the first data point y_1 and y_m is $O((\log_{10}(\delta^+)A_k)/2)$, and the area between y_m and δ is also $O((\log_{10}(\delta^+)A_k)/2)$.

Figure 8 and table 1 indicate that the integrals of the TKE production and dissipation are equally partitioned around y_m with a value of $1.25\ \ln(\delta^+)$. The advantage and importance of meso-scaled length can be summarized simply: at sufficiently high Reynolds number, the integrals of TKE production and dissipation are equally partitioned around the peak Reynolds shear stress location y_m.

The approximation of pre-multiplied TKE production or dissipation as a rectangle is crude, but it is interesting that meso-scaled distance from the wall reveals that the TKE production and dissipation seem to centre the integrals evenly across the meso-layer. Next we will use DNS data to assess quantitatively the partition of the integral of the TKE production and TKE dissipation around the peak Reynolds shear stress location y_m.

3.5. *Partition of the TKE production and dissipation around y_m*

Using the TKE budget data from DNS by Abe *et al.* (2001), Iwamoto *et al.* (2002), Lee & Moser (2015) and Pirozzoli *et al.* (2016), the integrals of TKE production from 0 to y_m and from y_m to δ are calculated and presented in figure 9(*a*). Also plotted is the $(U_b^+ - 9.13)/2$ from (3.1). To better show the partition, the integrals are divided by $(U_b^+ - 9.13)$ in figure 9(*b*), which clearly shows that at low Reynolds number, the integral from 0 to y_m is larger than that from y_m to δ. For example, at $Re_\tau = 100$, the value from 0 to y_m (solid green square) is approximately 0.6, and the value from

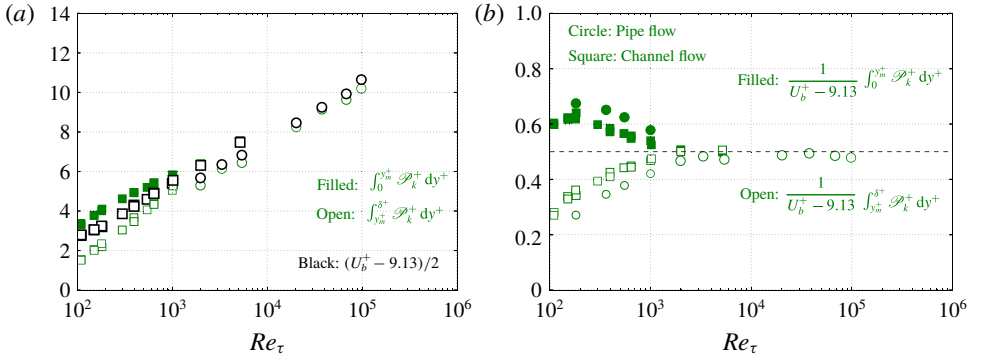

FIGURE 9. (Colour online) Partition of the integral of the TKE production about the peak Reynolds shear stress location y_m. (*a*) Integral of the TKE production from 0 to y_m and from y_m to δ versus Reynolds number. (*b*) Integrals divided by $(U_b^+ - 9.13)$ versus Reynolds number. The filled squares represent $\int_0^{y_m^+} \mathscr{P}_k^+ \,\mathrm{d}y^+$ calculated from DNS of turbulent channel flow by Abe *et al.* (2001), Iwamoto *et al.* (2002), Lee & Moser (2015). The open squares represent $\int_{y_m^+}^{\delta^+} \mathscr{P}_k^+ \,\mathrm{d}y^+$. Circles represent turbulent pipe flow data from El Khoury *et al.* (2013).

y_m to δ (open green square) is approximately 0.25. Note that they do not add up to 1 because $\int_0^{\delta^+} (\partial U^+/\partial y^+)^2 \,\mathrm{d}y^+$ is larger than 9.13 at this low Reynolds number. The dominance of the near-wall region at low Reynolds number is consistent with the observation of Marusic *et al.* (2010*a*).

At sufficiently high Reynolds number, figure 9(*b*) shows that the integral of TKE production indeed approaches an equal partition around y_m, with $\int_0^{y_m^+} \mathscr{P}_k^+ \,\mathrm{d}y^+ \approx \int_{y_m^+}^{\delta^+} \mathscr{P}_k^+ \,\mathrm{d}y^+ \approx 0.5(U_b^+ - 9.13)$.

Partition of the integral of TKE dissipation is calculated from DNS data and presented in figure 10. It can only be proven that the global integral of the TKE production must equal the global integral of the TKE dissipation in turbulent channel flows and turbulent pipe flows. Given the complicated roles of the transport terms in the different layers, it is not known *a priori* that the partition of the integral of the TKE dissipation will be the same as that of the TKE production. However, the DNS data shown in figure 10 strongly suggest that the integral of the TKE dissipation data is also equally partitioned around the peak Reynolds shear stress location y_m at sufficiently high Reynolds number, $\int_0^{y_m^+} \mathscr{E}_k^+ \,\mathrm{d}y^+ \approx \int_{y_m^+}^{\delta^+} \mathscr{E}_k^+ \,\mathrm{d}y^+ \approx 0.5(U_b^+ - 9.13)$.

3.6. *'Log layer' in the integral profiles of TKE production and dissipation*

Finally, we investigate the integral profiles of the TKE production and dissipation. Denote the integral of TKE production and dissipation as

$$\mathcal{I}_{\mathscr{P}_k}(y) = \int_0^y \mathscr{P}_k \,\mathrm{d}y; \quad \mathcal{I}_{\mathscr{E}_k}(y) = \int_0^y \mathscr{E}_k \,\mathrm{d}y. \tag{3.7a,b}$$

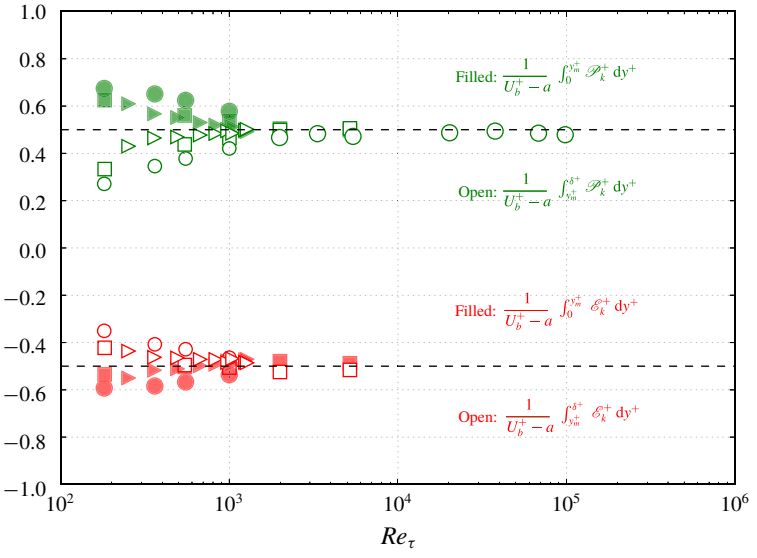

FIGURE 10. (Colour online) Partition of TKE production and dissipation around the peak Reynolds shear stress location y_m. Turbulent channel flows (squares), turbulent pipe flows (circles), ZPG TBL (triangles). A value of $a = 9.13$ is used for turbulent channel and pipe flows and $a = 12$ is used for ZPG TBL.

Using inner-scaled variables, the inner-scaled integral functions can be written as

$$\mathcal{I}^+_{\mathscr{P}_k}(y) = \frac{\displaystyle\int_0^y \mathscr{P}_k \,\mathrm{d}y}{u_\tau^3}; \quad \mathcal{I}^+_{\mathscr{E}_k}(y) = \frac{\displaystyle\int_0^y \mathscr{E}_k \,\mathrm{d}y}{u_\tau^3}. \tag{3.8a,b}$$

The integral profiles of TKE production and dissipation are calculated from the DNS data of turbulent channel flow by Abe *et al.* (2001) and Lee & Moser (2015) and presented in figure 11. Also plotted in the figure is the inner normalized mean streamwise velocity U^+ at $Re_\tau = 5200$ shifted downwards by 9.3 and the log-law equation for U^+, but with an additive constant of -4.3.

In the viscous sublayer and buffer layer, the integral of the TKE dissipation is larger than the integral of the TKE production. For example, the integral of the TKE production at $y^+ \approx 5$ (the end of the viscous sublayer) is $\int_0^5 \mathscr{P}_k^+ \,\mathrm{d}y^+ \approx 0.06$. The integral of the TKE dissipation at the end of viscous sublayer is $\int_0^5 \mathscr{E}_k^+ \,\mathrm{d}y^+ \approx 0.8$. As shown in figure 1(*a*), in the viscous sublayer the TKE production term is small, and the TKE dissipation is balanced by the viscous diffusion term.

Figure 12(*a*) shows the integral profiles of TKE production and dissipation for turbulent pipe flows, and figure 12(*b*) shows the same profiles for ZPG TBL. To facilitate comparison, the same logarithmic equation $(1/0.4)\ln(y^+) - 4.3$ is plotted in all three figures. Notable features in figures 11 and 12 are as follows. (i) At the channel or pipe centreline, the magnitude of the global integral of the TKE production is the same as that of the dissipation. However, outside the boundary layer of ZPG TBL, the magnitude of the global integral of TKE production is larger than that of the dissipation, as shown in figure 12(*b*). (ii) Although all three types

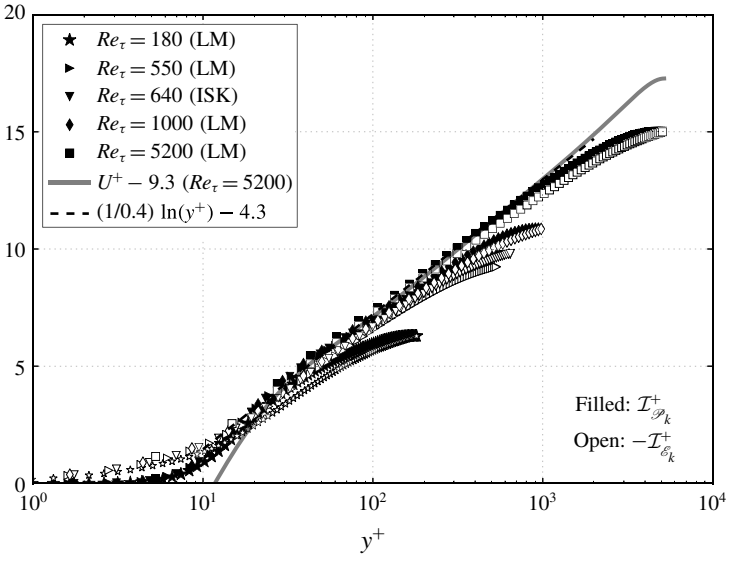

FIGURE 11. Integral profiles of the TKE production and dissipation versus y^+. Data are from DNS of turbulent channel flows by Iwamoto *et al.* (2002) and Lee & Moser (2015).

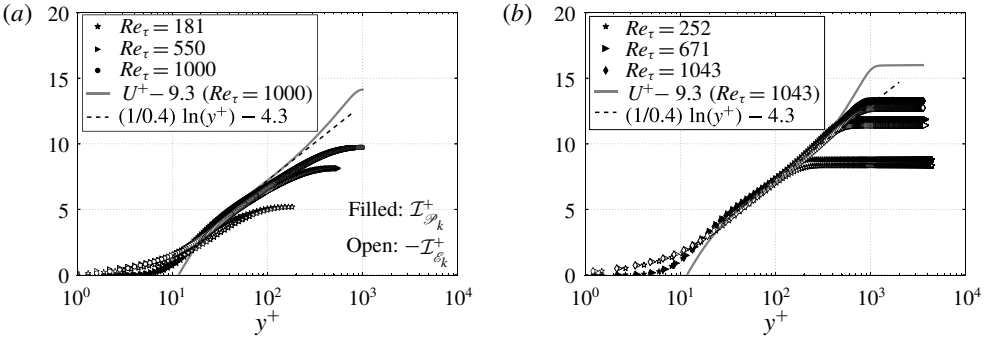

FIGURE 12. Integral profiles of the TKE production and dissipation versus y^+. (*a*) Turbulent pipe flows at $Re_\tau = 181$, 550, 1000 by El Khoury *et al.* (2013). (*b*) ZPG TBL at $Re_\theta = 670$, 2000, 3270 ($Re_\tau = 252$, 671, 1043) by Schlatter & Örlü (2010).

of turbulent wall-bounded flows exhibit a logarithmic-like layer at sufficiently high Reynolds number, noticeable differences exist among the three flows, especially in the wake region.

The logarithmic-like layer shown in figures 11 and 12 can be represented as

$$\mathcal{I}^+_{\mathscr{P}_k}(y^+) \approx \frac{1}{\kappa}\ln(y^+) + C_{\mathscr{P}_k}, \tag{3.9}$$

$$-\mathcal{I}^+_{\mathscr{E}_k}(y^+) \approx \frac{1}{\kappa}\ln(y^+) + C_{\mathscr{E}_k}. \tag{3.10}$$

The von Kármán 'constant' in the log law is approximately the same as the one in the U^+ profile. Discussions on the existence of the log layer and the 'universality' of

the von Kármán constant can be found in the work of Nagib & Chauhan (2008). The downward shift in the integral profiles of TKE production and dissipation is directly related to the constant -9.13 in the global integral identity equation (3.1).

The logarithmic-like behaviour of the TKE production integral in turbulent channel flow can be explained by (2.10):

$$\mathcal{I}^+_{\mathscr{P}_k}(y^+) = U^+ - \left\{ \frac{y^+U^+ - \int_0^{y^+} U^+\,\mathrm{d}y^+}{\delta^+} + \int_0^{y^+} \left(\frac{\partial U^+}{\partial y^+}\right)^2 \mathrm{d}y^+ \right\}. \tag{3.11}$$

Thus the integral of TKE production can be approximated by U^+ with a downward shift. It has been shown above that, at sufficiently high Reynolds number, $\int_0^{y^+} (\partial U^+/\partial y^+)^2\,\mathrm{d}y^+ \lesssim 9.13$. Moreover, outside the viscous sublayer and buffer layer, it can be shown that $(y^+U^+ - \int_0^{y^+} U^+\,\mathrm{d}y^+)/\delta^+$ is small. In other words, the logarithmic-like behaviour of the TKE production is directly related to the logarithmic-like behaviour of the mean velocity U^+.

The logarithmic-like scaling for the global integrals of the TKE production and dissipation, equation (3.1), is also directly related to the logarithmic-like behaviour of the integral profiles of TKE production and dissipation, equations (3.9) and (3.10). At sufficiently high Reynolds number, equations (3.9) and (3.10) indicate that

$$\int_0^{\delta^+} \mathscr{P}_k^+\,\mathrm{d}y^+ \approx \frac{1}{\kappa}\ln(\delta^+) + C_{\mathscr{P}_k} = O(\ln(\delta^+)), \tag{3.12}$$

$$\int_0^{\delta^+} -\mathscr{E}_k^+\,\mathrm{d}y^+ \approx \frac{1}{\kappa}\ln(\delta^+) + C_{\mathscr{E}_k} = O(\ln(\delta^+)). \tag{3.13}$$

It is known that, at sufficiently high Reynolds number, $y_m = O(\delta\nu/u_\tau)$ or $y_m^+ = O(\sqrt{\delta^+})$. From (3.9) and (3.10), the scaling for the integral of TKE production and dissipation from wall to y_m can be estimated as

$$\int_0^{y_m^+} \mathscr{P}_k^+\,\mathrm{d}y^+ \approx \frac{1}{\kappa}\ln(\sqrt{\delta^+}) + C_{\mathscr{P}_k} = O(0.5\ln(\delta^+)) \approx 0.5\int_0^{\delta^+} \mathscr{P}_k^+\,\mathrm{d}y^+, \tag{3.14}$$

$$\int_0^{y_m^+} -\mathscr{E}_k^+\,\mathrm{d}y^+ \approx \frac{1}{\kappa}\ln(\sqrt{\delta^+}) + C_{\mathscr{E}_k} = O(0.5\ln(\delta^+)) \approx 0.5\int_0^{\delta^+} -\mathscr{E}_k^+\,\mathrm{d}y^+. \tag{3.15}$$

Hence, the equal partition of TKE production around y_m is also directly related to the logarithmic-like behaviour of the integral profiles of TKE production and dissipation, equation (3.9).

The noticeable difference among the integrals of the TKE production and dissipation in channel flows, pipe flows and ZPG TBL is similar to the differences observed in the low-order statistics on different types of turbulent wall-bounded flows, in particular within the wake region, as discussed by Jiménez *et al.* (2009), Mathis *et al.* (2009*b*), Monty *et al.* (2009) and Ng *et al.* (2011). The differences between the internal flow (channel or pipe flows) and ZPG TBL are traced by Jiménez *et al.* (2009) to an excess of production of the streamwise turbulent energy in the outer part of the boundary layer.

4. Discussion

The integral properties of the TKE production and dissipation revealed in the present work may provide quantitative measures of the inner and outer interactions and the emergence of the second peak in the streamwise variance. For example, it has been reported by Marusic *et al.* (2017) that a second peak in the streamwise variance appears when $Re_\tau \gtrapprox 15\,000$–$20\,000$, which roughly corresponds to two decades of scale separation on both sides of y_m in figure 8, $l_m/l_\nu \sim 100$ and $\delta/l_m \sim 100$. Furthermore, the reported location of the second $\langle uu \rangle$ peak scales as the meso-length scale $O(l_m)$ as shown in Mathis, Hutchins & Marusic (2009*a*), Ng *et al.* (2011), and Vincenti *et al.* (2013), not as the outer scale δ.

Interestingly, Tsuji (1999) has found that the peak position of the dissipation spectrum in turbulent boundary layers scales the same as the peak Reynolds shear stress location. In other words, both peak locations scale not with inner length scale l_ν, nor with outer length scale l_o, but with the meso-length scale l_m.

The integrals of TKE production and dissipation exhibit a logarithmic-like layer in turbulent wall-bounded flows, similar to that for the mean streamwise velocity U^+. In the viscous sublayer, the mean streamwise velocity grows almost linearly, $U^+ \approx y^+$. In contrast, the integrals of TKE production and dissipation grow much more slowly in the viscous sublayer and buffer layer. As a result, the integral of TKE production and dissipation approaches an equal partition at relatively moderate Reynolds numbers of $Re_\tau \approx 1000$–2000 (see figure 9). Wei *et al.* (2005) have shown that the velocity increment ΔU would establish an equal partition around the peak Reynolds shear stress location at much higher Reynolds number. This is because U_c^+ or U_∞^+ grows nearly logarithmically with Reynolds number, so the velocity increment within the viscous sublayer and buffer layer of $\Delta U^+ \approx 12$ becomes negligible only at very high Reynolds number. The partition of velocity increment reflects the distribution of mean vorticity within the boundary layer, which is important in understanding the structure and underlying physics in turbulent wall-bounded flows.

5. Conclusions

Direct numerical simulation and high resolution experimental data of turbulent wall-bounded flows (channel, pipe, ZPG TBL) have been used to investigate the integral properties of the turbulent-kinetic-energy production and dissipation. We first verified the RD identity for the global integral of the TKE production for turbulent channel flows, turbulent pipe flows and ZPG TBL. For channel flows, the global integral identity for the TKE production is $\int_0^{\delta^+} \mathscr{P}_k^+ \,\mathrm{d}y^+ = U_b^+ - \int_0^{\delta^+} (\partial U^+/\partial y^+)^2 \,\mathrm{d}y^+$. At low Reynolds number, the global integral $\int_0^{\delta^+} (\partial U^+/\partial y^+)^2 \,\mathrm{d}y^+$ is larger than the global integral of the TKE production. As Reynolds number increases, $\int_0^{\delta^+} (\partial U^+/\partial y^+)^2 \,\mathrm{d}y^+$ decreases to a constant value of 9.13 for turbulent channel flows, and the global integral of the TKE production can be approximated as $\int_0^{\delta^+} \mathscr{P}_k^+ \,\mathrm{d}y^+ \approx U_b^+ - 9.13$ for turbulent channel flows. It is observed that at sufficiently high Reynolds number, both U_b^+ and the global integral of TKE production and dissipation can be well approximated by a logarithmic function.

The partition of the TKE production and dissipation can be better shown if the pre-multiplied TKE production and dissipation are plotted versus meso-scaled distance from the wall y/l_m on semilogarithmic axes. At sufficiently high Reynolds number, it is found that the integrals of TKE production and dissipation are equally partitioned around the peak Reynolds shear stress location y_m. This equal partition underlines the

important role of the meso-length scale l_m in the dynamics of turbulent wall-bounded flows.

At sufficiently high Reynolds number, the integral profiles of the TKE production and dissipation are found to exhibit a logarithmic-like layer similar to that of the mean streamwise velocity U^+. The logarithmic-like behaviour of the integral profiles of TKE production and dissipation, the equal partition of the integrals around y_m, and the logarithmic-like scaling for the global integrals of the TKE production and dissipation are intimately related.

Acknowledgements

The author is very grateful to Dr Abe, Dr Bernardini, Dr De Graaff, Dr Eaton, Dr Iwamoto, Dr Jimenez, Dr El Khoury, Dr Hoyas, Dr Hultmark, Dr Kasagi, Dr Kawamura, Dr Lee, Dr Moser, Dr Orlu, Dr Pirozzoli, Dr Schlatter, Dr Simens, Dr Smits and Dr Vallikivi for generously sharing their data.

Appendix A. Derivation of the global identity for TBL

The mean momentum balance (MMB) equation for two-dimensional incompressible turbulent boundary layer flow reads

$$0 = \left[U\frac{\partial V}{\mathrm{d}y} - V\frac{\partial U}{\mathrm{d}y}\right] + \nu\frac{\partial^2 U}{\partial y^2} + \frac{\partial R_{12}}{\partial y} - \frac{1}{\rho}\frac{\mathrm{d}P}{\mathrm{d}x}. \tag{A 1}$$

Note that the mean continuity equation is used to replace $\partial U/\partial x$ by $-\partial V/\partial y$, so all the derivatives are local. The corresponding boundary conditions are

$$y = 0 \text{ (wall)}: \quad U = 0, \quad V = 0, \quad R_{12} = 0, \quad \nu\frac{\partial U}{\partial y} = u_\tau^2. \tag{A 2a–d}$$

$$y = \delta \text{ (boundary layer edge)}: \quad U = U_e, \quad V = V_e, \quad R_{12} = 0. \tag{A 3a–c}$$

Integrating the MMB equation (A 1) in the wall-normal direction and applying boundary conditions produces a relation for the total shear stress as

$$\nu\frac{\partial U}{\partial y} + R_{12} = u_\tau^2 - \int_0^y \left[U\frac{\partial V}{\mathrm{d}y} - V\frac{\partial U}{\mathrm{d}y}\right]\mathrm{d}y + \frac{1}{\rho}\frac{\mathrm{d}P}{\mathrm{d}x}y. \tag{A 4}$$

Step one in obtaining integral of TKE production is to multiply the MMB equation (A 1) by a weight function U:

$$0 = \left[U\frac{\partial V}{\mathrm{d}y} - V\frac{\partial U}{\mathrm{d}y}\right]U + \nu\frac{\partial^2 U}{\partial y^2}U + \frac{\partial R_{12}}{\partial y}U - \frac{1}{\rho}\frac{\mathrm{d}P}{\mathrm{d}x}U, \tag{A 5}$$

then integration of the weighted equation (A 5) in the wall-normal direction yields

$$\begin{aligned} 0 \;=\; & \int_0^y \left[U\frac{\partial V}{\mathrm{d}y} - V\frac{\partial U}{\mathrm{d}y}\right]U\,\mathrm{d}y + \left\{\nu\frac{\partial U}{\partial y}U - \nu\int_0^y \left(\frac{\partial U}{\partial y}\right)^2 \mathrm{d}y\right\} \\ & + \left\{R_{12}U - \int_0^y R_{12}\frac{\partial U}{\partial y}\,\mathrm{d}y\right\} - \frac{1}{\rho}\frac{\mathrm{d}P}{\mathrm{d}x}\int_0^y U\,\mathrm{d}y. \end{aligned} \tag{A 6}$$

Note that integration by parts is applied to the second and third terms in (A 5). Substituting the relation for the total shear stress in (A 4), the integral of TKE production can be expressed as

$$\begin{aligned}\int_0^y \mathscr{P}_k \,\mathrm{d}y \;=\; & u_\tau^2 U \\ & + \left\{ \int_0^y U \left[U\frac{\partial V}{\mathrm{d}y} - V\frac{\partial U}{\mathrm{d}y} \right] \mathrm{d}y - U \int_0^y \left[U\frac{\partial V}{\mathrm{d}y} - V\frac{\partial U}{\mathrm{d}y} \right] \mathrm{d}y \right\} \\ & + \frac{1}{\rho}\frac{\mathrm{d}P}{\mathrm{d}x} \left\{ yU - \int_0^y U \,\mathrm{d}y \right\} - \nu \int_0^y \left(\frac{\partial U}{\partial y} \right)^2 \mathrm{d}y, \end{aligned} \tag{A 7}$$

and the global integral identity for TKE production can be expressed as

$$\begin{aligned}\int_0^\delta \mathscr{P}_k \,\mathrm{d}y \;=\; & u_\tau^2 U_e \\ & + \left\{ \int_0^\delta U \left[U\frac{\partial V}{\mathrm{d}y} - V\frac{\partial U}{\mathrm{d}y} \right] \mathrm{d}y - U_e \int_0^\delta \left[U\frac{\partial V}{\mathrm{d}y} - V\frac{\partial U}{\mathrm{d}y} \right] \mathrm{d}y \right\} \\ & + \frac{1}{\rho}\frac{\mathrm{d}P}{\mathrm{d}x} \left\{ \delta U_e - \int_0^\delta U \,\mathrm{d}y \right\} - \nu \int_0^\delta \left(\frac{\partial U}{\partial y} \right)^2 \mathrm{d}y. \end{aligned} \tag{A 8}$$

The integral of TKE production in inner scaling becomes

$$\begin{aligned}\int_0^{y^+} \mathscr{P}_k^+ \,\mathrm{d}y^+ \;=\; & U^+ + \left\{ \int_0^{y^+} U^+ \left[U^+\frac{\partial V^+}{\mathrm{d}y^+} - V^+\frac{\partial U^+}{\mathrm{d}y^+} \right] \mathrm{d}y^+ \right. \\ & \left. - U^+ \int_0^{y^+} \left[U^+\frac{\partial V^+}{\mathrm{d}y^+} - V^+\frac{\partial U^+}{\mathrm{d}y^+} \right] \mathrm{d}y^+ \right\} \\ & + \left[\frac{\nu}{u_\tau^3}\frac{1}{\rho}\frac{\mathrm{d}P}{\mathrm{d}x} \right] \left\{ y^+U^+ - \int_0^{y^+} U^+ \,\mathrm{d}y^+ \right\} - \int_0^{y^+} \left(\frac{\partial U^+}{\partial y^+} \right)^2 \mathrm{d}y^+, \end{aligned} \tag{A 9}$$

and the global integral of TKE production in inner scaling becomes

$$\begin{aligned}\int_0^{\delta^+} \mathscr{P}_k^+ \,\mathrm{d}y^+ \;=\; & U_e^+ + \left\{ \int_0^{\delta^+} U^+ \left[U^+\frac{\partial V^+}{\mathrm{d}y^+} - V^+\frac{\partial U^+}{\mathrm{d}y^+} \right] \mathrm{d}y^+ \right. \\ & \left. - U_e^+ \int_0^{\delta^+} \left[U^+\frac{\partial V^+}{\mathrm{d}y^+} - V^+\frac{\partial U^+}{\mathrm{d}y^+} \right] \mathrm{d}y^+ \right\} \\ & + \left[\frac{\nu}{u_\tau^3}\frac{1}{\rho}\frac{\mathrm{d}P}{\mathrm{d}x} \right] \left\{ \delta^+U_e^+ - \int_0^{\delta^+} U^+ \,\mathrm{d}y^+ \right\} - \int_0^{\delta^+} \left(\frac{\partial U^+}{\partial y^+} \right)^2 \mathrm{d}y^+. \end{aligned} \tag{A 10}$$

In ZPG TBL, the mean pressure gradient is zero, so the terms involved $\mathrm{d}P/\mathrm{d}x$ will be zero in (A 9) and (A 10).

Appendix B. Derivation of the global identity for turbulent pipe flows

The mean momentum balance equation for fully developed turbulent pipe flows reads

$$0 = \frac{2u_\tau^2}{R} + \frac{1}{r}\frac{\partial}{\partial r}\left(\nu r\frac{\partial U}{\partial r}\right) + \frac{1}{r}\frac{\partial}{\partial r}(rR_{12}). \tag{B 1}$$

Note that $(2u_\tau^2/R)$ comes from the mean pressure gradient $-(1/\rho)(\mathrm{d}P/\mathrm{d}x)$ (see Pope 2001). The corresponding boundary conditions are

$$r = 0 \text{ (centre)}: \quad U = U_c, \quad R_{12} = 0, \quad \nu\frac{\partial U}{\partial r} = 0; \tag{B 2a–c}$$

$$r = R \text{ (wall)}: \quad U = 0, \quad R_{12} = 0, \quad \nu\frac{\partial U}{\partial r} = -u_\tau^2. \tag{B 3a–c}$$

Integration of the MMB equation (B 1) along the r direction, $\int_0^r(\mathrm{MMB})2\pi r\,\mathrm{d}r$, yields a relation for the total shear stress as

$$\nu\frac{\partial U}{\partial r} + R_{12} = -\frac{u_\tau^2}{R}r. \tag{B 4}$$

Note that in the cylindrical coordinate system r starts from the centreline. As a result, both the viscous shear stress $\nu\partial U/\partial r$ and the Reynolds shear stress R_{12} are negative. This equation is used to calculate R_{12} in the superpipe using the measured U data.

Step one in obtaining the integral of TKE production is to multiply the MMB equation (B 1) by a weight function U

$$0 = \frac{2u_\tau^2}{R}U + \frac{1}{r}\frac{\partial}{\partial r}\left(\nu r\frac{\partial U}{\partial r}\right)U + \frac{1}{r}\frac{\partial}{\partial r}(rR_{12})U. \tag{B 5}$$

In step two, integration of the weighted equation (B 5), $\int_0^r(\mathrm{MMB})U2\pi r\,\mathrm{d}r$, along the r direction yields

$$0 = \frac{2u_\tau^2}{R}\int_0^r rU\,\mathrm{d}r + \left\{\nu r\frac{\partial U}{\partial r}U - \nu\int_0^r r\left(\frac{\partial U}{\partial r}\right)^2\mathrm{d}r\right\} + \left\{rR_{12}U - \int_0^r rR_{12}\frac{\partial U}{\partial r}\,\mathrm{d}r\right\}. \tag{B 6}$$

Substituting the relation for the total shear stress in (B 4), the integral of TKE production can be rearranged as

$$\int_0^r rR_{12}\frac{\partial U}{\partial r}\,\mathrm{d}r = \frac{u_\tau^2}{R}\left\{2\int_0^r rU\,\mathrm{d}r - r^2U\right\} - \nu\int_0^r r\left(\frac{\partial U}{\partial r}\right)^2\mathrm{d}r. \tag{B 7}$$

Setting $r = R$ in (B 7) yields the global integral identity of TKE production for pipe flows

$$\int_0^R rR_{12}\frac{\partial U}{\partial r}\,\mathrm{d}r = u_\tau^2U_bR - \nu\int_0^R r\left(\frac{\partial U}{\partial r}\right)^2\mathrm{d}r. \tag{B 8}$$

The integral equation (B 7) in inner scaling can be expressed as

$$\int_0^{r^+} r^+R_{12}^+\frac{\partial U^+}{\partial r^+}\,\mathrm{d}r^+ = \frac{\left(2\displaystyle\int_0^{r^+} r^+U^+\,\mathrm{d}r^+ - r^{+2}U^+\right)}{R^+} - \int_0^{r^+} r^+\left(\frac{\partial U^+}{\partial r^+}\right)^2\mathrm{d}r^+, \tag{B 9}$$

and the inner-scaled global integral identity for TKE production in pipe flow can be expressed as

$$\int_0^{R^+} r^+ R_{12}^+ \frac{\partial U^+}{\partial r^+}\,\mathrm{d}r^+ = U_b^+ R^+ - \int_0^{R^+} r^+ \left(\frac{\partial U^+}{\partial r^+}\right)^2 \mathrm{d}r^+. \tag{B 10}$$

For the convenience of comparison with channel flow and TBL flow, pipe flow data are often presented versus distance from the pipe surface $y = R - r$. Hence, $\partial U/\partial y = -\partial U/\partial r$. From (B 4), it can be easily shown that the Reynolds shear stress in turbulent pipe flows can be expressed as

$$R_{12} = -\left(u_\tau^2 - \frac{u_\tau^2}{R} y - \nu \frac{\partial U}{\partial y}\right). \tag{B 11}$$

For turbulent channel flow, the Reynolds shear stress can be obtained from (2.5) as

$$R_{12} = u_\tau^2 - \frac{u_\tau^2}{\delta} y - \nu \frac{\partial U}{\partial y}. \tag{B 12}$$

Thus the Reynolds shear stress in turbulent pipe flow and turbulent channel flow have the same function form, but opposite sign, due to the designation of the positive wall-normal direction.

REFERENCES

ABE, H. & ANTONIA, R. A. 2009 Near-wall similarity between velocity and scalar fluctuations in a turbulent channel flow. *Phys. Fluids* **21** (2), 025109.

ABE, H. & ANTONIA, R. A. 2016 Relationship between the energy dissipation function and the skin friction law in a turbulent channel flow. *J. Fluid Mech.* **798**, 140–164.

ABE, H. & ANTONIA, R. A. 2017 Relationship between the heat transfer law and the scalar dissipation function in a turbulent channel flow. *J. Fluid Mech.* **830**, 300–325.

ABE, H., KAWAMURA, H. & MATSUO, Y. 2001 Direct numerical simulation of a fully developed turbulent channel flow with respect to the Reynolds number dependence. *Trans. ASME J. Fluids Engng* **123** (2), 382–393.

AFZAL, N. 1982 Fully developed turbulent flow in a pipe: an intermediate layer. *Arch. Appl. Mech.* **52** (6), 355–377.

AFZAL, N. 1984 Mesolayer theory for turbulent flows. *AIAA J.* **22** (3), 437–439.

BERNARDINI, M., PIROZZOLI, S. & ORLANDI, P. 2014 Velocity statistics in turbulent channel flow up to $Re_\tau = 4000$. *J. Fluid Mech.* **742**, 171–191.

CANTWELL, B. J. 1981 Organized motion in turbulent flow. *Annu. Rev. Fluid Mech.* **13** (1), 457–515.

DE GRAAFF, D. B. & EATON, J. K. 2000 Reynolds-number scaling of the flat-plate turbulent boundary layer. *J. Fluid Mech.* **422**, 319–346.

EGGELS, J. G. M., UNGER, F., WEISS, M. H., WESTERWEEL, J., ADRIAN, R. J., FRIEDRICH, R. & NIEUWSTADT, F. T. M. 1994 Fully developed turbulent pipe flow: a comparison between direct numerical simulation and experiment. *J. Fluid Mech.* **268**, 175–210.

EL KHOURY, G. K., SCHLATTER, P., NOORANI, A., FISCHER, P. F., BRETHOUWER, G. & JOHANSSON, A. V. 2013 Direct numerical simulation of turbulent pipe flow at moderately high Reynolds numbers. *Flow Turbul. Combust.* **91** (3), 475–495.

FERNHOLZ, H. H. & FINLEY, P. J. 1996 The incompressible zero-pressure-gradient turbulent boundary layer: an assessment of the data. *Prog. Aerosp. Sci.* **32** (4), 245–311.

FIFE, P., KLEWICKI, J., MCMURTRY, P. & WEI, T. 2005*a* Multiscaling in the presence of indeterminacy: wall-induced turbulence. *Multiscale Model. Simul.* **4** (3), 936–959.

FIFE, P., WEI, T., KLEWICKI, J. & MCMURTRY, P. 2005*b* Stress gradient balance layers and scale hierarchies in wall-bounded turbulent flows. *J. Fluid Mech.* **532**, 165–189.

FUKAGATA, K., IWAMOTO, K. & KASAGI, N. 2002 Contribution of Reynolds stress distribution to the skin friction in wall-bounded flows. *Phys. Fluids* **14** (11), L73–L76.

GAD-EL HAK, M. & BANDYOPADHYAY, P. R. 1994 Reynolds number effects in wall-bounded turbulent flows. *Appl. Mech. Rev.* **47** (8), 307–365.

HOYAS, S. & JIMÉNEZ, J. 2008 Reynolds number effects on the Reynolds-stress budgets in turbulent channels. *Phys. Fluids* **20** (10), 101511.

HULTMARK, M., VALLIKIVI, M., BAILEY, S. & SMITS, A. 2012 Turbulent pipe flow at extreme Reynolds numbers. *Phys. Rev. Lett.* **108** (9), 094501.

HULTMARK, M., VALLIKIVI, M., BAILEY, S. & SMITS, A. 2013 Logarithmic scaling of turbulence in smooth-and rough-wall pipe flow. *J. Fluid Mech.* **728**, 376–395.

IWAMOTO, K., SUZUKI, Y. & KASAGI, N. 2002 Reynolds number effect on wall turbulence: toward effective feedback control. *Intl J. Heat Fluid Flow* **23** (5), 678–689.

JIMÉNEZ, J. 2013 Near-wall turbulence. *Phys. Fluids* **25** (10), 101302.

JIMÉNEZ, J., HOYAS, S., SIMENS, M. P. & MIZUNO, Y. 2009 Comparison of turbulent boundary layers and channels from direct numerical simulation. In *TSFP Digital Library Online*. Begel House Inc.

JIMÉNEZ, J., HOYAS, S., SIMENS, M. P. & MIZUNO, Y. 2010 Turbulent boundary layers and channels at moderate Reynolds numbers. *J. Fluid Mech.* **657**, 335–360.

KLEWICKI, J. C. 2010 Reynolds number dependence, scaling, and dynamics of turbulent boundary layers. *Trans. ASME J. Fluids Engng* **132** (9), 094001.

LAADHARI, F. 2007 Reynolds number effect on the dissipation function in wall-bounded flows. *Phys. Fluids* **19** (3), 038101.

LEE, M. & MOSER, R. D. 2015 Direct numerical simulation of turbulent channel flow up to $Re = 5200$. *J. Fluid Mech.* **774**, 395–415.

LONG, R. R. & CHEN, T.-C. 1981 Experimental evidence for the existence of the mesolayer in turbulent systems. *J. Fluid Mech.* **105**, 19–59.

MARUSIC, I., BAARS, W. J. & HUTCHINS, N. 2017 Scaling of the streamwise turbulence intensity in the context of inner-outer interactions in wall turbulence. *Phys. Rev. Fluids* **2** (10), 100502.

MARUSIC, I., MATHIS, R. & HUTCHINS, N. 2010*a* High Reynolds number effects in wall turbulence. *Intl J. Heat Fluid Flow* **31** (3), 418–428.

MARUSIC, I., MCKEON, B. J., MONKEWITZ, P. A., NAGIB, H. M., SMITS, A. J. & SREENIVASAN, K. R. 2010*b* Wall-bounded turbulent flows at high Reynolds numbers: recent advances and key issues. *Phys. Fluids* **22** (6), 065103.

MATHIS, R., HUTCHINS, N. & MARUSIC, I. 2009*a* Large-scale amplitude modulation of the small-scale structures in turbulent boundary layers. *J. Fluid Mech.* **628**, 311–337.

MATHIS, R., MONTY, J. P., HUTCHINS, N. & MARUSIC, I. 2009*b* Comparison of large-scale amplitude modulation in turbulent boundary layers, pipes, and channel flows. *Phys. Fluids* **21** (11), 111703.

MONTY, J. P., HUTCHINS, N., NG, H., MARUSIC, I. & CHONG, M. S. 2009 A comparison of turbulent pipe, channel and boundary layer flows. *J. Fluid Mech.* **632**, 431–442.

NAGIB, H. M. & CHAUHAN, K. A. 2008 Variations of von Kármán coefficient in canonical flows. *Phys. Fluids* **20** (10), 101518.

NG, H., MONTY, J., HUTCHINS, N., CHONG, M. S. & MARUSIC, I. 2011 Comparison of turbulent channel and pipe flows with varying Reynolds number. *Exp. Fluids* **51** (5), 1261–1281.

ORLANDI, P. 1997 Helicity fluctuations and turbulent energy production in rotating and non-rotating pipes. *Phys. Fluids* **9** (7), 2045–2056.

PANTON, R. L. 2001 Overview of the self-sustaining mechanisms of wall turbulence. *Prog. Aerosp. Sci.* **37** (4), 341–383.

PERRY, A. E., MARUSIC, I. & JONES, M. B. 2002 On the streamwise evolution of turbulent boundary layers in arbitrary pressure gradients. *J. Fluid Mech.* **461**, 61–91.

PIROZZOLI, S., BERNARDINI, M. & ORLANDI, P. 2016 Passive scalars in turbulent channel flow at high Reynolds number. *J. Fluid Mech.* **788**, 614–639.

POPE, S. B. 2001 *Turbulent Flows*. Cambridge University Press.

RENARD, N. & DECK, S. 2016 A theoretical decomposition of mean skin friction generation into physical phenomena across the boundary layer. *J. Fluid Mech.* **790**, 339–367.

ROBINSON, S. K. 1991 Coherent motions in the turbulent boundary layer. *Annu. Rev. Fluid Mech.* **23** (1), 601–639.

SCHLATTER, P. & ÖRLÜ, R. 2010 Assessment of direct numerical simulation data of turbulent boundary layers. *J. Fluid Mech.* **659**, 116–126.

SIMENS, M. P., JIMÉNEZ, J., HOYAS, S. & MIZUNO, Y. 2009 A high-resolution code for turbulent boundary layers. *J. Comput. Phys.* **228** (11), 4218–4231.

SMITS, A. J. & MARUSIC, I. 2013 Wall-bounded turbulence. *Phys. Today* **66** (9), 25–30.

SMITS, A. J., MCKEON, B. J. & MARUSIC, I. 2011 High-Reynolds number wall turbulence. *Annu. Rev. Fluid Mech.* **43**, 353–375.

SREENIVASAN, K. R. 1989 The turbulent boundary layer. In *Frontiers in Experimental Fluid Mechanics*, pp. 159–209. Springer.

SREENIVASAN, K. R. & SAHAY, A. 1997 The persistence of viscous effects in the overlap region, and the mean velocity in turbulent pipe and channel flows. In *Self-Sustaining Mechanisms of Wall Turbulence* (ed. R. Panton), Advances in Fluid Mechanics, vol. 15, pp. 253–272. Computational Mechanics Publications, Southampton, UK.

TSUJI, Y. 1999 Peak position of dissipation spectrum in turbulent boundary layers. *Phys. Rev.* E **59** (6), 7235.

VALLIKIVI, M., HULTMARK, M. & SMITS, A. J. 2015 Turbulent boundary layer statistics at very high Reynolds number. *J. Fluid Mech.* **779**, 371–389.

VINCENTI, P., KLEWICKI, J., MORRILL-WINTER, C., WHITE, C. M. & WOSNIK, M. 2013 Streamwise velocity statistics in turbulent boundary layers that spatially develop to high Reynolds number. *Exp. Fluids* **54** (12), 1629.

WEI, T., FIFE, P., KLEWICKI, J. & MCMURTRY, P. 2005 Properties of the mean momentum balance in turbulent boundary layer, pipe and channel flows. *J. Fluid Mech.* **522**, 303–327.

WEI, T. & WILLMARTH, W. W. 1989 Reynolds-number effects on the structure of a turbulent channel flow. *J. Fluid Mech.* **204**, 57–95.

WOSNIK, M., CASTILLO, L. & GEORGE, W. K. 2000 A theory for turbulent pipe and channel flows. *J. Fluid Mech.* **421**, 115–145.

WU, X. & MOIN, P. 2009 Direct numerical simulation of turbulence in a nominally zero-pressure-gradient flat-plate boundary layer. *J. Fluid Mech.* **630**, 5–41.

ZANOUN, E.-S., NAGIB, H. & DURST, F. 2009 Refined cf relation for turbulent channels and consequences for high-Re experiments. *Fluid Dyn. Res.* **41** (2), 021405.